Russian Journal of Earth Sciences

Special Issue: "Advances in Environmental Studies, from the VIII International Scientific and Practical Conference 'Fundamental and Applied Aspects of Geology, Geophysics and Geoecology Using Modern Information Technologies' "

Wave Climate of the Barents Sea Based on Satellite Altimetry Data

S. A. Lebedev[1, 2, 3,*], A. G. Kostianoy[1, 2, 4, 5], E. A. Kostianaia[1, 4], A. V. Bocharov[1, 2, 4, 6], and A. O. Slobodyanyuk[3]

[1] Geophysical Center, Russian Academy of Sciences, Moscow, Russia
[2] Maykop State Technological University, Maykop, Russia
[3] National Research University Moscow Institute of Electronic Technology, Zelenograd, Russia
[4] Shirshov Institute of Oceanology, Russian Academy of Sciences, Moscow, Russia
[5] S. Yu. Witte Moscow University, Moscow, Russia
[6] Tver State University, Tver, Russia
* **Correspondence to:** Sergey Lebedev, s.lebedev@gcras.ru

The paper is devoted to the study of the Barents Sea wave climate, which was built on the basis of satellite altimetry data provided by ERS-1/2, GFO-1, Envisat, Cryosat-2, SARAL, Sentinel-3a/3b. A special statistical procedure has been applied to obtain a single dataset of Significant Wave Height (SWH) variability relative to ERS-1 satellite altimetry measurements for 1991–2021. This is the first time such a wind wave database has been created for the Barents Sea. For this time period a monthly mean SWH interannual trend was equal to +0.10 ± 0.06 m/decade. Seasonal variability of SWH interannual trends varies from +0.05 m/decade in March to +0.15 m/decade in September. Values of SWH trends over +0.12 m/decade are observed from July to November which is explained by steady interannual reduction of ice cover in the Barents Sea and by a significant increase in storm activity in the region. The obtained results show that, on the one hand, significant reduction in ice cover in the Barents Sea allows ice-free navigation for a longer time during a year, especially in Autumn, but on the other hand it increases wind fetch, which along with a significant increase in storm activity in the Barents Sea will lead to an increase of wind wave height in the Barents Sea. This will represent potential difficulties (and even danger) to navigation of ships designed for navigation in ice conditions and not intended for navigation in open waters of the world's oceans where large waves may be observed (e.g., icebreakers, barges, and other vessels).

Keywords: Barents Sea, Significant Wave Height (SWH), wave climate, satellite altimetry, GEOSAT, ERS-1/2, GFO-1, Envisat, Cryosat-2, SARAL, Sentinel-3a/3b.

Citation: Lebedev S. A., Kostianoy A. G., Kostianaia E. A., Bocharov A. V., and Slobodyanyuk A. O. (2025), Wave Climate of the Barents Sea Based on Satellite Altimetry Data, *Russian Journal of Earth Sciences*, 25, ES6007, EDN: IEMJCZ, https://doi.org/10.2205/2025ES001076

Research Article

Received: 2025-09-10
Accepted: 2025-11-10
Published: 2025-12-10

Introduction

The Barents Sea is a key western section of the Northern Sea Route (NSR), home to the largest ice-free port of Murmansk and the largest rail and road hub in northwestern European Russia. It also provides access to the Port of Arkhangelsk in the White Sea. The dynamics of cargo traffic through the ports of Murmansk and Arkhangelsk is directly linked to the growth of cargo turnover along the NSR and shows an upward trend [*Kuznetsova and Vasilyeva*, 2024].

The development of the Arctic shelf and the NSR have entailed numerous additional requirements for the composition, completeness, and reliability of data on hydrometeorological conditions, and particularly on the wave climate of the Arctic seas, which is of vital

importance for maritime safety during shipping operations. Adverse weather conditions, such as rough seas, are a major risk factor for both personnel and cargo handling operations, including loading, stowage and securing cargo onboard ships. Severe weather, in particular rough seas can pose risks to cargo safety as well. Such data is particularly necessary for areas where in situ observations are either not conducted or are conducted extremely rarely.

The Barents Sea is one of the most studied seas on the Russian Arctic shelf, with systematic oceanographic and meteorological research conducted there since the early 20th century [*Kostianoy et al.*, 2004; *Rodionov and Kostianoy*, 1998]. However, instrumental studies of wave conditions have been sporadic until recently, because this is done at several weather stations located along the coasts of the Barents Sea. Wave conditions in the central part of the sea remains unknown, as well as changes in wave climate related to ice cover retreat due to regional climate change.

The only continuous and large-scale source of wave climate information is visual ship observations of wind waves [*Freeman et al.*, 2016]. These observations are considered unreliable, subject to human error, and poorly suited for statistical analysis due to the uneven density of observations and the low accuracy of wave parameter estimates. However, visual observations are currently the longest-running and provide independent estimates of wind wave heights. Every day, 30-40 reports are received for each of the main synoptic periods in the Barents Sea, primarily from fishing vessels. Their distribution across the sea depends on fishing conditions, with the greatest number of observations occurring in the southwestern part of the sea. Today wave observations from voluntary observing ships (VOS) play an important role in building wave climate databases in the World Ocean [*Collins et al.*, 2025; *Gavrikov et al.*, 2016; *Grigorieva and Badulin*, 2016; *Gulev and Grigorieva*, 2004; *Gulev et al.*, 2003].

Data from specialized wave moored buoys is more informative. Currently, two such buoys of the Norwegian Meteorological Institute are operating on the border of the Norwegian and Barents Seas near Bear Island and two near the coast of Norway [*Orimolade and Gudmestad*, 2017].

In 2024, during the "European Arctic 2024: Geological Record of Environmental and Climate Change" expedition (cruise 96 of the R/V Akademik Mstislav Keldysh), a permanent weather buoy, the Sea-Air-Wave Station (SAWS), developed at the P.P. Shirshov Institute of Oceanology of the Russian Academy of Sciences (Moscow, Russia), was deployed for the first time in the northeastern Barents Sea. In the upper ocean layer, the buoy measures wave characteristics, temperature, salinity, acidity (pH), and CO_2 concentration [*Sharmar et al.*, 2025].

However, data from ship observations and buoy measurements are insufficient for a comprehensive study of the wave climate in the Barents Sea. In addition to this information, wave characteristics are calculated using discrete spectral models WAM [*Reistad et al.*, 2011], WAVEWATCH III [*Tsarau et al.*, 2020], and SWAN [*Myslenkov et al.*, 2015]. Frequency-directed spectra are calculated for a given wind field or atmospheric pressure, and from them, wave heights and periods are calculated. The capabilities of model wave calculations for long periods of time (years and decades) have been significantly expanded due to reanalysis data from meteorological parameters (NCEP/NCAP, ERA, MERRA, etc.) [*Compo et al.*, 2011]. Since 2000, the Russian Maritime Register of Shipping has used this approach in preparing and creating reference data on the wind and wave regime of the seas of Russia [*Lopatukhin et al.*, 2013, 2003].

Polar mesocyclones play a special role in the atmosphere of Arctic latitudes. They are characterized by a short lifetime (less than a day) and relatively small characteristic sizes (with a diameter of less than 1000 km). Because the characteristic sizes and lifetimes of polar mesocyclones are smaller than those of synoptic-scale atmospheric vortices, they are not always detected in the atmospheric reanalysis data. It should also be noted that the meteorological observation network in the high latitudes of the Northern Hemisphere is quite sparse. In particular, in the Barents Sea, weather stations are located along the coasts

of the mainland, Svalbard, Franz Josef Land Archipelago, and Novaya Zemlya. A vast sea area of about 1000 × 1000 km remains without any wind wave measurements.

Therefore, satellite altimetry data are the only representative information on Significant Wave Heights (SWH) in the waters of Russia's Arctic seas, and in the Barents Sea in particular. Since the GlobWave database [*Timmermans et al.*, 2020], which includes altimetry measurements from the ERS-1/2, Envisat, TOPEX/Poseidon, Jason-1/2/3, GEOSAT Follow-ON (GFO-1), Cryosat-2 and SARAL satellites, is limited to the time interval 1991–2017, additional information from satellites operating from 2017 to the present is required to refine the wave regime of the Barents Sea.

This paper aims to study seasonal and interannual variability and statistics of SWH based on satellite altimetry data derived from GEOSAT, ERS-1/2, GFO-1, Envisat, Cryosat-2, SARAL, Sentinel-3a/3b from 1991 to 2021. These data were combined into a single series of observations. The obtained results are compared with interannual variability of ice cover and storm activity in the Barents Sea.

Research Area

The Barents Sea is one of the shelf Arctic seas. It is located on the continental European shelf between the northern coast of Europe and three archipelagoes – Novaya Zemlya, Franz Josef Land, and Spitsbergen (Svalbard) (Figure 1). Its open water area is approximately 1,424,000 km^2 and total volume is 322,000 km^3. The Barents Sea shelf is rather deep. More than 50% of the area has a depth of 200–500 m. The average depth is 222 m; the maximum depth in the Norwegian trench reaches 513 m and in the Franz Josef Land straits it exceeds 600 m [*Atlas…*, 1985; *Kostianoy et al.*, 2004; *Rodionov and Kostianoy*, 1998]. The Barents Sea watershed area is 668,000 km^2. The total river runoff is 163 km^3/year; 80–90% of it falls on the southeastern region of the sea. The largest river flowing into the Barents Sea is the Pechora River which has about a half of the watershed area, i.e., 322,000 km^2; its runoff is 130 km^3/year. The river runoff is essentially reflected in hydrological conditions only in the southeastern part of the sea. Therefore, this area is sometimes referred to as the Pechora Sea [*Hydrometeorological…*, 1985; *Hydrometeorology…*, 1990].

Strong and prolonged winds cause surging fluctuations in the level of the Barents Sea. They are most significant (up to 3 m) along the Kola coast and Svalbard (about 1 m), smaller values (up to 0.5 m) are observed off the coast of Novaya Zemlya and in the southeastern part of the sea [*Hydrometeorology…*, 1990]. Waves in the Arctic seas depend on the wind regime and sea ice conditions. In general, the ice regime in the Arctic Ocean is unfavorable for the development of wave processes. The irregular coastline, the presence of numerous islands, as well as strong tidal currents have a significant influence on the propagation of wind waves and swell. The latter, in the case of waves propagating towards the currents, can increase the wave height by more than two times. Currents in the same direction, on the contrary, reduce the height by one and a half times. The Barents Sea is one of the stormiest in the World Ocean. In winter, storm events develop here, in the open sea the height of wind waves reaches 10–11 m. The highest waves in the southeastern part of the sea are formed by northerly and northeasterly winds, their height can exceed 10 m [*Hydrometeorology…*, 1990].

Storm wave zones in the Barents Sea are generally formed when deep cyclones from the Norwegian Sea or the Scandinavian Peninsula enter the sea [*Nesterov*, 2015]. During the 18 most powerful storms between 1955 and 1985, according to ship observations, wave heights were 8–10 m, but according to calculations, they could have reached 11–13 m [*Hydrometeorology…*, 1990].

Data and Methods

The SWH value is obtained from altimetry data after using an analytical retracking algorithm (processing the shape of the reflected pulse), for example Ocean-1/2 [*Amarouche et al.*, 2004; *Brown*, 1977; *Hayne*, 1980]. Verification of remote sensing data against in situ measurement data showed the accuracy of SWH calculations to be 10% [*Bué et al.*, 2024;

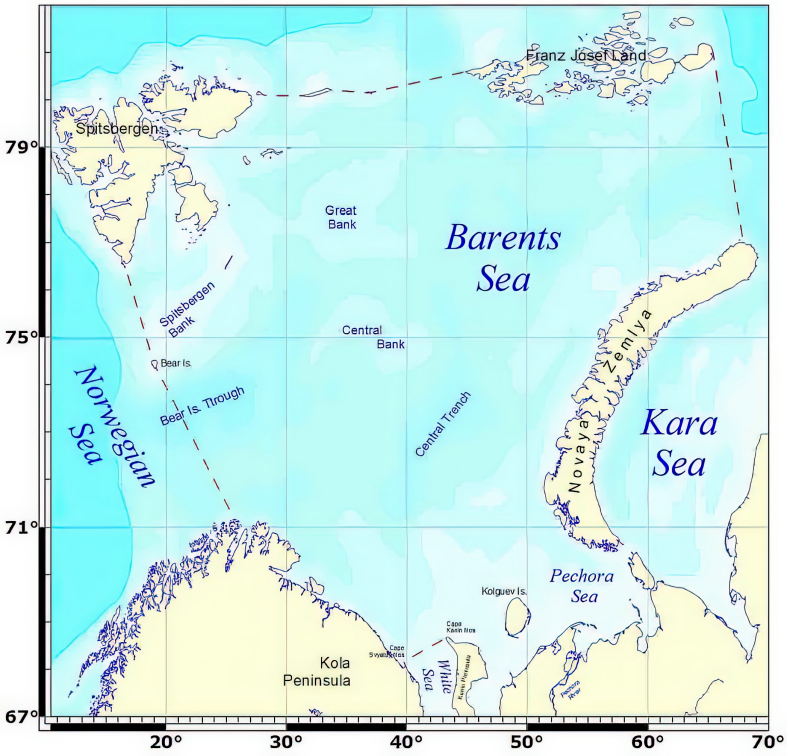

Figure 1. Map of the Barents Sea. The red dashed line shows the boundaries of the Barents Sea [*Lebedev et al.*, 2010].

Liu et al., 2016; *López-García et al.*, 2019; *Meucci et al.*, 2020], which in turn made it possible to use them to verify the results of model calculations or vice versa [*Cabral et al.*, 2022; *Lebedev and Gusev*, 2022; *Myslenkov et al.*, 2017; *Reistad et al.*, 2011].

For the Barents Sea only those satellite missions which have orbital inclinations greater than 66.5° (GEOSAT, ERS-1/2, GFO-1, Envisat, Cryosat-2, SARAL, Sentinel-3a/3b) were selected from the numerous altimetry missions. These satellites include Synthetic Aperture Radars. In this case, nadir measurements were selected. Figure 2 shows interannual variability of monthly average SWH values for 1985–2021 starting from GEOSAT in 1985 to SARAL and Sentinel-3a/3b measurements till the end of 2021. GEOSAT data were not included in further analysis because of the data gap between GEOSAT and ERS-1 missions (see Figure 2 and Table 1). Spatial coverage of the above mentioned satellite groundtracks (without GEOSAT) over the Barents Sea for March and September in 1993–2021 is presented in Figure 3.

The number of measurements for each satellite and mission characteristics are presented in Table 1. For the Exact Repeat Missions (ERM) programs, the cycle duration is indicated as well. For our study, we calculated monthly average SWH values over the entire ice-free water area of the Barents Sea. Table 1 clearly shows that the time intervals of altimetry measurements from all satellites overlap. However, the monthly average SWH data within the overlap interval do not coincide (Figure 2), due to differences in the density and timing of measurements, as well as in the retracking algorithm and its software implementation. Combining all the data into a single time series as an extension of the ERS-1 satellite's altimetry measurements requires special processing, and GEOSAT data will not be used.

Analysis of SWH climate variability requires combining data from different satellites against "reference" measurements. In [*Liu et al.*, 2016], altimetry data were calibrated against measurements from moored wave buoys during the summer season. Altimetry measurements taken at distances of less than 50 km from the buoys and time intervals of

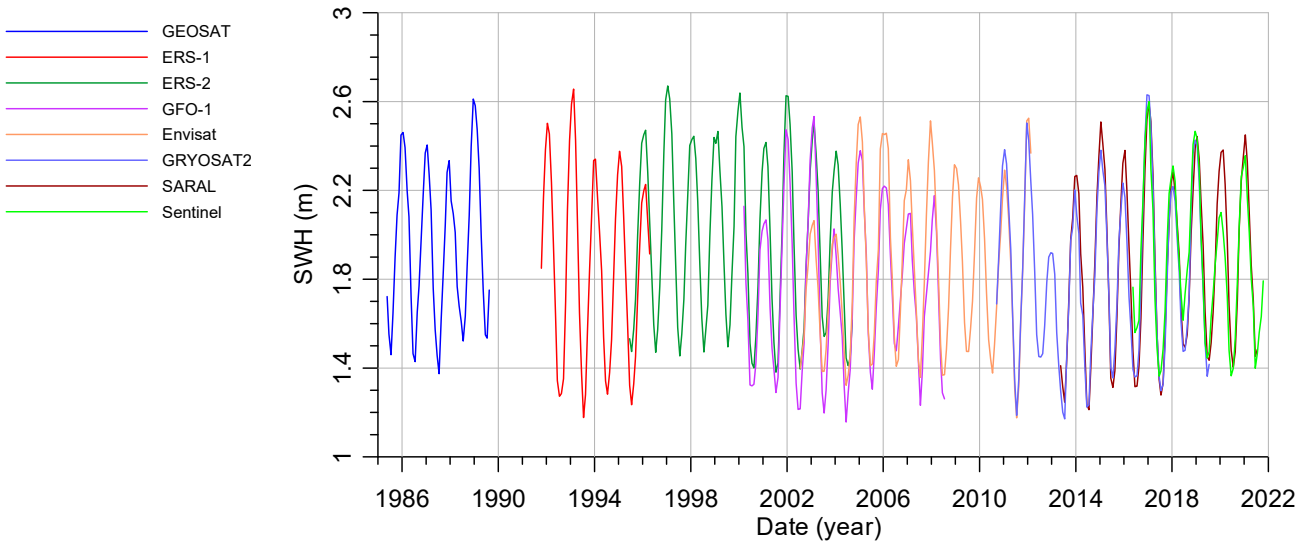

Figure 2. Interannual variability of monthly average SWH values for 1985–2021, smoothed by a median filter, in the Barents Sea for various altimetry measurement programs presented in Table 1.

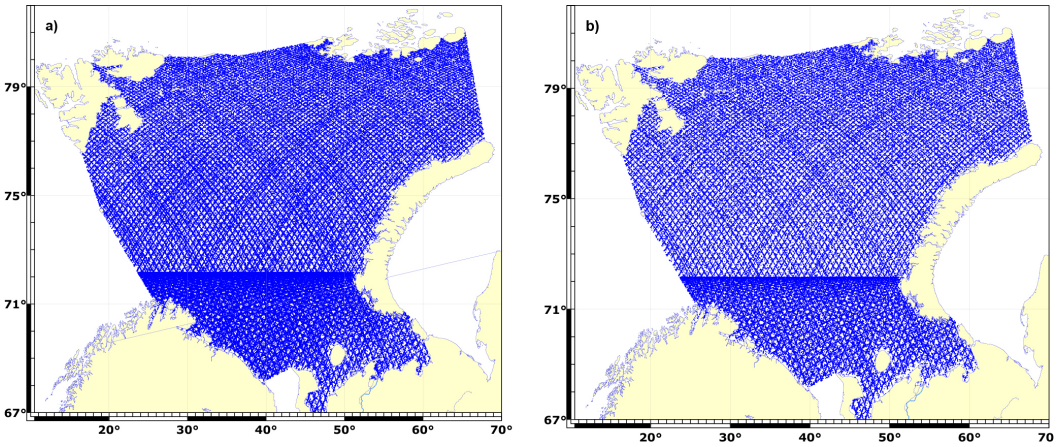

Figure 3. Spatial coverage of the ERS-1/2, GFO-1, Envisat, Cryosat-2, SARAL, Sentinel-3a/3b satellite groundtracks (without GEOSAT) over the Barents Sea for March (473,056 measurements) (a) and September (689,693 measurements) (b) in 1993–2021.

less than 1 hour were considered. In the present study, in the absence of buoy measurements, data from the ERS-1 satellite are proposed as the "reference" measurements.

To combine the data into a single time series relative to ERS-1 measurements, the following values were calculated:

- average SWH, measured by first satellite and second satellite:

$$\mathrm{MSWH}_{1\text{ or }2} = \frac{1}{N}\sum_{i=1}^{N}\mathrm{SWH}_i,$$

- average deviation of a difference between measurements by the first and second satellite (Mean Error – ME or bias):

$$\mathrm{ME} = \frac{1}{N}\sum_{i=1}^{N}\left(\mathrm{SWH}_{1,i} - \mathrm{SWH}_{2,i}\right),$$

Table 1. Satellite altimetry data used in this research, mission characteristics and the number of measurements in the Barents Sea

Satellite	Phase	Time period, month/year	Orbital inclination, degree	Revisit period, days	Number of measurements
GEOSAT	Phase A	03/1985 – 11/1986	108	–	353,508
	Phase B	11/1986 – 12/1989		17	
ERS-1	Phase A	07/1991 – 11/1991	98.5	3	744,507
	Phase B	11/1991 – 03/1992		3	
	Phase C	04/1992 – 12/1993		35	
	Phase D	12/1993 – 04/1994		3	
	Phase E	04/1994 – 09/1994		–	
	Phase F	09/1994 – 03/1995		–	
	Phase G	04/1995 – 06/1996		35	
ERS-2		04/1995 – 06/2002	98.6	35	
GFO-1		02/1998 – 09/2008	108	17	1,206,955
Envisat		03/2002 – 04/2012	98.6	35	1,686,096
Cryosat-2		04/2010 – 12/2021	92	–	249,302
SARAL	Phase A	03/2013 – 06/2016	98.5	35	959,830
	Phase B	07/2016 – 12/2021			
Sentinel 3A		02/2016 – 12/2021	98.6	27	494,754
Sentinel 3B		04/2018 – 12/2021	98.6	27	
Total:					5,694,952

- Standard Deviation (SD) of a difference between measurements by the first and second satellite:

$$\mathrm{SD} = \sqrt{\frac{1}{N-1}\sum_{i=1}^{N}\left(\mathrm{SWH}_{1,i} - \mathrm{SWH}_{2,i} - \mathrm{ME}\right)^2},$$

- Root Mean Square Error (RSME):

$$\mathrm{RMSE} = \sqrt{\mathrm{ME}^2 + \mathrm{SD}^2},$$

- Scatter Index (SI):

$$\mathrm{SI} = \mathrm{RMSE} \Big/ \mathrm{MSWH}_1,$$

- Correlation coefficient (R):

$$\mathrm{R} = \frac{\sum_{i=1}^{N}\left(\mathrm{SWH}_{1,i} - \mathrm{MSWH}_1\right)\left(\mathrm{SWH}_{2w,i} - \mathrm{MSWH}_{2,i}\right)}{\sqrt{\sum_{i=1}^{N}\left(\mathrm{SWH}_{1,i} - \mathrm{MSWH}_1\right)^2\left(\mathrm{SWH}_{2w,i} - \mathrm{MSWH}_{2,i}\right)^2}},$$

- Coefficients a and b of a linear regression:

$$\mathrm{FSWH}_2 = b + a \cdot \mathrm{SWH}_1,$$

- Coefficient of determination (R^2):

$$R^2 = 1 - \sum_{i-1}^{N} (SWH_{2,i} - FSWH_2)^2 \Big/ \sum_{i-1}^{N} (SWH_{1,i} - SWH_{2,i})^2.$$

where $FSWH_2$ – value of SWH, calculated based on the linear regression. In the case of two variables, the coefficient of determination is equal to the square of the correlation coefficient.

The results of calculations of these statistical characteristics are presented in Table 2. The climatic trend of SWH variability was calculated based on the results of linear regression.

Table 2. Results of statistical analysis of satellite altimetry data in the Barents Sea for the intervals of intersection of measurements of different satellites, which were used to combine the data into a single time series relative to the altimetry measurements of the ERS-1 satellite

Satellite	Statistical parameters									
	$MSWH_1$	$MSWH_2$	ME	SD	RMSE	SI	R	*b*	*a*	R^2
ERS–1 ERS–2	1.74	1.98	−0.25	0.04	0.25	0.14	0.9967	−0.20	0.9764	0.9935
ERS–2 GFO–1	1.70	1.76	0.13	0.23	0.26	0.15	0.9359	0.14	0.8850	0.8759
ERS-2 Envisat	1.61	1.67	−0.06	0.20	0.21	0.13	0.9334	−0.51	1.2709	0.8713
Envisat CRYOSAT–2	2.17	1.91	0.26	0.28	0.39	0.18	0.9341	−0.07	1.1744	0.8726
Cryosat-2 SARAL	2.04	1.84	0.20	0.22	0.30	0.15	0.9471	−0.01	1.1157	0.8970
SARAL Sentinel-3	2.08	1.89	0.19	0.31	0.37	0.18	0.8415	0.26	0.9651	0.7082

Results

The results of combining altimetry data from various satellites into a single SWH time series relative to the ERS-1 satellite measurements based on statistical analysis (Table 2) are presented in Figure 4. For the period 1991–2021, according to the average annual data, the SWH interannual trend was equal to +0.10 ± 0.06 m/decade. A SWH maximum is observed during winter time when stronger winds blow over the Barents Sea. During 1991–2021 we have observed several cases when SWH exceeded 3 m – in 1993, 2006, 2012, 2015, 2016 and 2017. Since 2017, maximum SWH values have been decreasing.

Before combining the satellite data into a single time series for the period from 1991 to 2021, the trend was negative and amounted to a statistically significant value of −0.30 ± 0.07 m/decade. After combining, it amounted to a statistically insignificant value of +0.10 ± 0.06 m/decade.

This is in good agreement with the results of [*Liu et al.*, 2016]. The trend magnitude obtained in this study was calculated using data from the ERS-2, Envisat, and CryoSat-2 satellites for the time interval 1996–2015 for two summer months August and September, when the ice cover in the Barents Sea is minimal [*Dumanskaya*, 2021] and, consequently, wind fetch is maximal.

The slight positive trend in SWH of +0.10 ± 0.06 m/decade that we obtained is due to a reduction in the annual sea ice extent in the Barents Sea. Over the past 50 years, ice formation dates have shifted later by 4–11 days, while ice-free sea dates have shifted earlier by an average of 5–13 days. The duration of the ice period has decreased by an average of 2–3 weeks [*Dumanskaya*, 2021]. A general decrease of ice cover is observed in the direction to the north-east, in the region between Franz Josef Land and Novaya Zemlya.

Based on the average annual SWH values (Figure 4), three periods can be distinguished: 1992–2007, 2007–2017, and 2017–2021 (Figure 5). During the first time interval, the interannual SWH trend was −0.020 ± 0.003 m/decade, which is statistically insignificant, and it can be considered that SWH did not change. During the next 10 years, from 2007

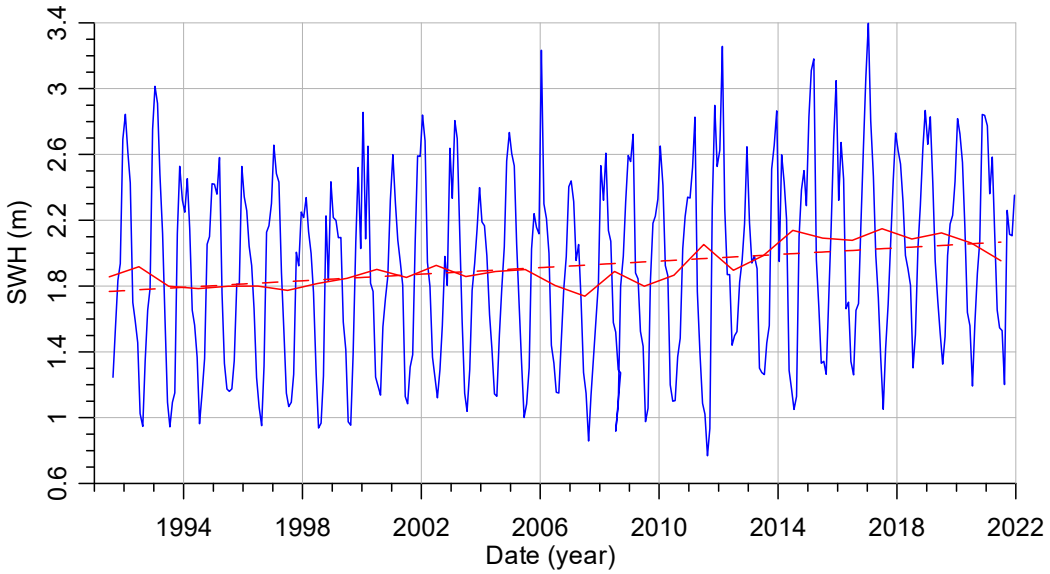

Figure 4. Interannual variability of monthly (blue line) and annual (red line) mean SWH values in the Barents Sea, combined into a single time series relative to ERS-1 satellite altimetry measurements for the period 1991–2021. The red dashed line shows the linear trend of +0.10 ± 0.06 m/decade.

to 2017, SWH increased at a rate of +0.310 ± 0.232 m/decade, and from 2017 to 2021, the SWH value increased at a statistically insignificant rate of +0.080 ± 0.005 m/decade. Between 2017 and 2018 there was a significant drop in SWH by 0.7 m.

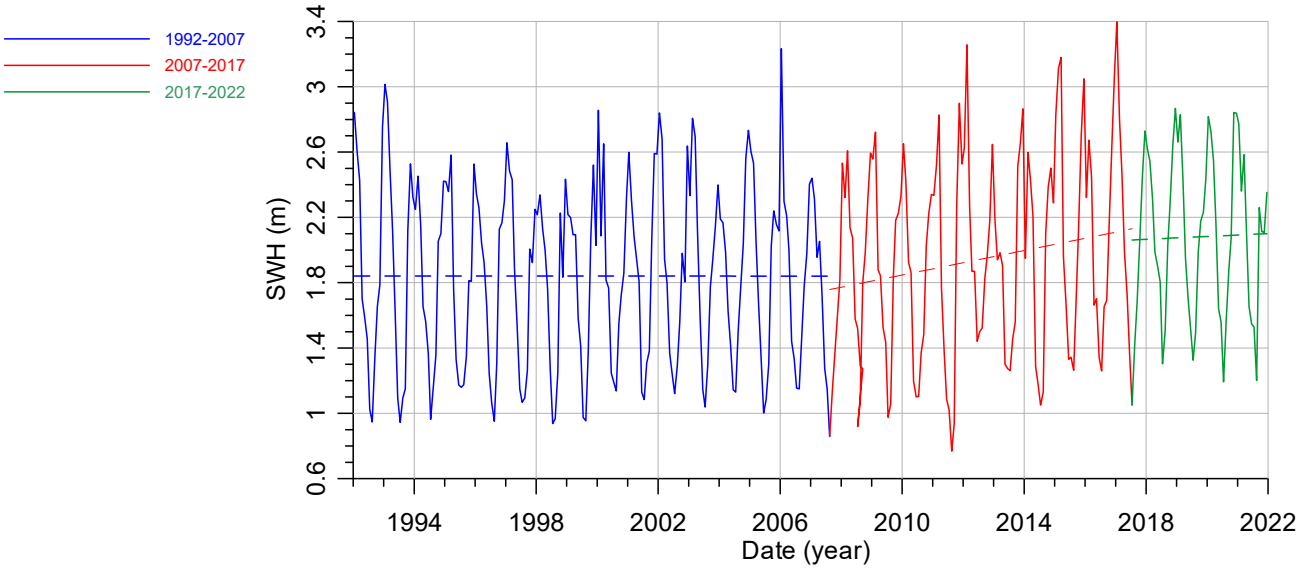

Figure 5. Interannual variability of monthly (blue line) and annual (red line) mean SWH values in the Barents Sea, combined into a single time series relative to altimetry measurements of the ERS-1 satellite for the period 1992–2021.

According to [*Mohamed et al.*, 2022], global warming has had a significant impact on the sea ice condition in the Barents Sea due to changes in air and water temperatures [*Serykh and Kostianoy*, 2019]. According to the Operational SST and Sea Ice Analyses (OSTIA) dataset [*Good et al.*, 2020] for the period 1982–2020, a significant decrease in the sea ice extent amounted to −6.52 ± 0.78%/decade and a shortening of the sea ice season by approximately 26.1 ± 7.5 day/decade, which led to an increase in the duration of the summer ice-free period by 3.4 months over the past 39 years. The sea ice area decreased

especially sharply in 2007, and the decreasing trend remained the same [*Mohamed et al.*, 2022].

According to [*Trofimov*, 2021], from 1991 to 2020, the ice extent of the Barents Sea, expressed as a percentage of the sea area covered by ice, was generally steadily declining. A statistically significant negative trend was observed, with the average annual ice extent decreasing by an average of −6.7%/decade (Figure 6). In 2016, the sea ice extent reached its minimum values since 1951, averaging 14.5% for the year against the norm of 34.3%. From 2016 to 2020, the ice extent was below the long-term average in all months but was nevertheless increasing at a rate of +16.8%/decade, and the wind fetch began to decrease (Figure 6). The latter is in good agreement with the SWH interannual variability (Figure 5), when in the winter of 2017/2018 SWH dropped after the maximum value in the winter of 2016/2017.

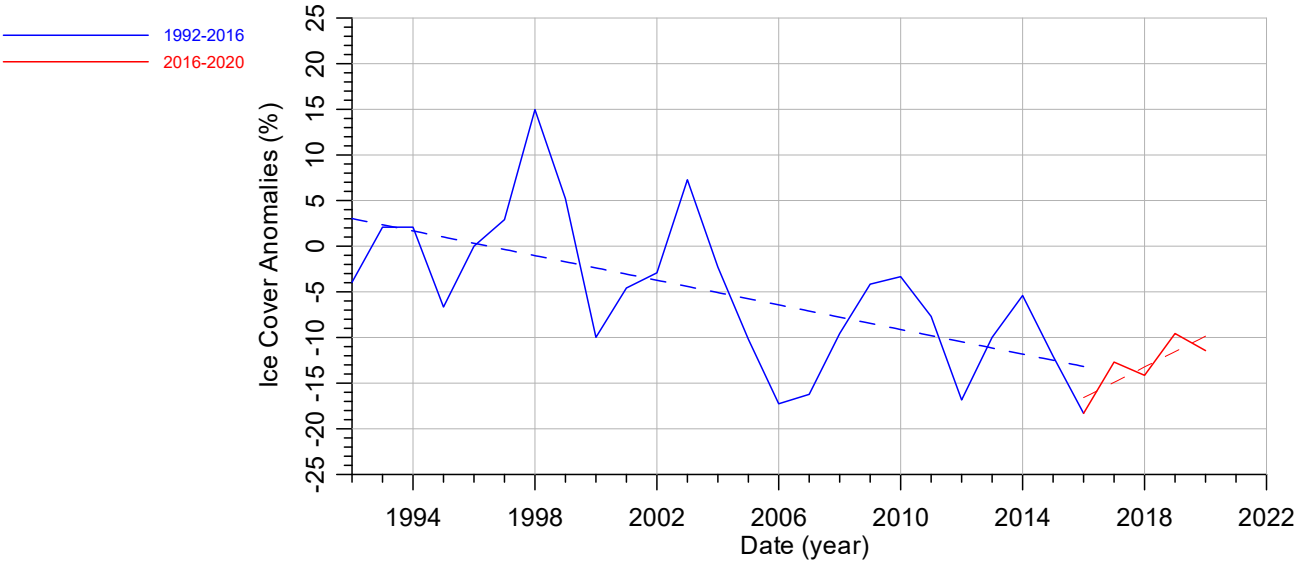

Figure 6. Interannual variability of ice coverage anomalies in the Barents Sea from 1992 to 2016 (blue line) and from 2016 to 2020 (red line) according to [*Trofimov*, 2021]. Dashed lines show linear trends.

Atmospheric circulation patterns resulted in abnormally high storm activity between 1992 and 2022, defined as the number of days with gale-force winds (15 m/s or greater). In the Barents Sea, 15 storm days per year are considered as the statistical norm. Three periods with positive trends in storm frequency anomalies were identified for 1992–2022: 1992–2007 with +19.7 days/decade, 2007–2017 with +25.7 days/decade, and 2017–2022 with +11.3 days/decade (Figure 7) [*Trofimov*, 2021], which, in general, is consistent with periods of SWH increasing (Figure 5). Thus, interannual SWH variability depends on both atmospheric forcing and ice coverage.

Seasonal variability of SWH in the Barents Sea is shown in Figure 8. The maximum of SWH according to satellite altimetry data is observed in winter – from November to March (Figure 8a, b), for example, in December – 2.38 ± 0.18 m, January – 2.43 ± 0.19 m and February – 2.35 ± 0.18 m. This is in accordance with the maximum wind speed over the Barents Sea. According to buoy data [*Orimolade and Gudmestad*, 2017; *Timmermans et al.*, 2020] located near the boundary of the Norwegian and Barents Seas, westerly and southwesterly waves with SWH > 3 m predominate in winter. Extreme waves of about 5 m are also observed during this season [*Nesterov*, 2020]. This is due to the fact that in winter, long-period swell from the Norwegian Sea comes to the Barents Sea [*Liu et al.*, 2016].

Minimum of SWH is observed in summer (Figure 8a, b), for example, in June – 1.42 ± 0.13 m, July – 1.37 ± 0.16 m and August – 1.48 ± 0.15 m. This is explained by light winds during this season, although the ice-free area is at its maximum. According to the wind rose at the island meteorological stations of Amderma, Barentsburg, Malye Kar-

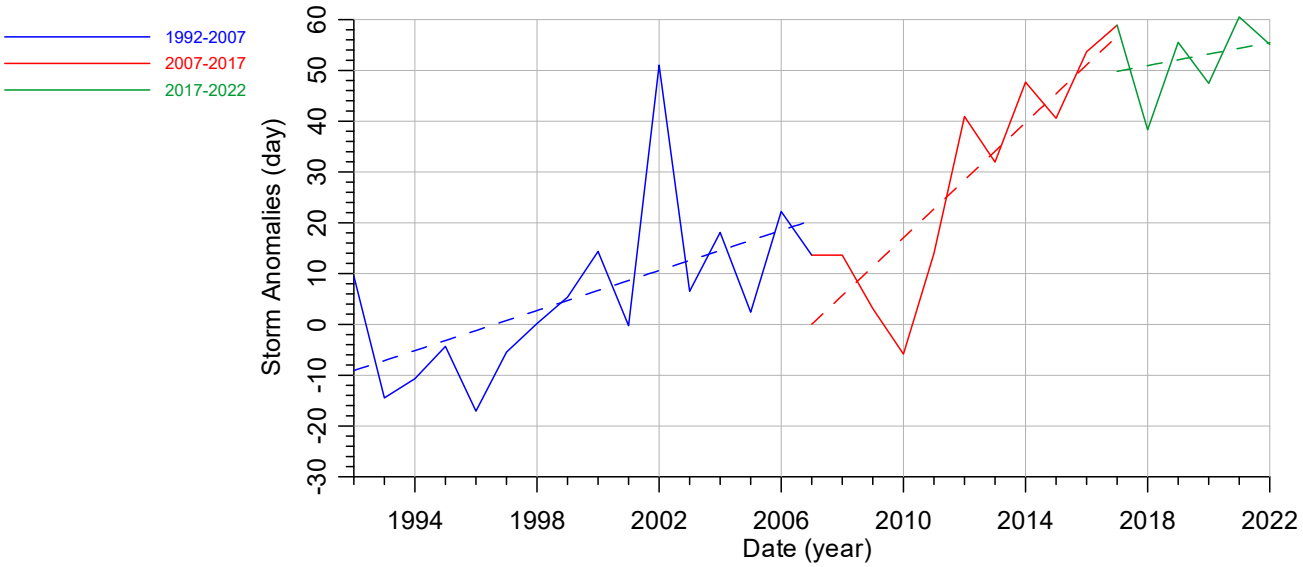

Figure 7. Interannual variability of storm anomalies (the number of stormy days with winds over 15 m/s over or below the norm of 15 stormy days per year) in the Barents Sea from 1992 to 2022 according to [*Trofimov*, 2021].

makuly, and Kolguyev Severny, southerly and southeasterly winds prevail during this season [*Myslenkov et al.*, 2015].

Seasonal variability of SWH interannual trends (Figure 8c) varies from +0.05 m/decade in March to +0.15 m/decade in September. Values of SWH trends over +0.12 m/decade are observed from July to November which is explained by a steady interannual reduction of ice cover in the Barents Sea and by a significant increase in storm activity in the region (Figure 7).

To analyze extreme waves in the Barents Sea using altimetry data, SWH distributions were calculated for each year (Figure 9). For the entire period from 1992 to 2022, the SWH distribution corresponds to the classical Rayleigh distribution (Figure 9a). The SWH frequency maximum is observed at 1.25 m, while the maximal SWH is of 8 m (Figure 9a).

$$f\,(\mathrm{SWH}) = \frac{\mathrm{SWH}}{\mathrm{SD}^2_{\mathrm{SWH}}} \exp\left(-\frac{\mathrm{SWH}^2}{2 \cdot \mathrm{SD}^2_{\mathrm{SWH}}}\right),$$

where $\mathrm{SD}_{\mathrm{SWH}}$ – standard deviation of SWH, which is of 1.1 m for the Barents Sea.

Extreme values of the wave height in the Barents Sea are generally considered to be greater than 5 m [*Nesterov*, 2015]. According to model calculations, maximum extreme waves of 18.1 m and 25.5 m are observed once every 50 years with a 3% and 0.1% probability, respectively, while 19.0 m and 26.8 m occur once every 100 years [*Lopatukhin et al.*, 2013, 2003].

The frequency of occurrence of storm surges of varying heights in the Barents Sea can be analyzed based on the variability of the SWH distribution for each year (Figure 9b). According to the data obtained, the highest number of anomalous SWH waves > 5 m was observed in 2014 and 2019, while the minimum was observed in 1993 and 1997.

Conclusions

The paper discusses the study of the Barents Sea wave climate, which was based on satellite altimetry data provided by ERS–1/2, GFO-1, Envisat, Cryosat–2, SARAL, Sentinel–3a/3b. A special statistical procedure has been applied to obtain a single dataset of Significant Wave Height (SWH) variability relative to ERS-1 satellite altimetry measurements for 1991–2021. This is the first time such a wind wave database has been created for the Barents Sea. The SWH maximum is observed during wintertime when stronger winds

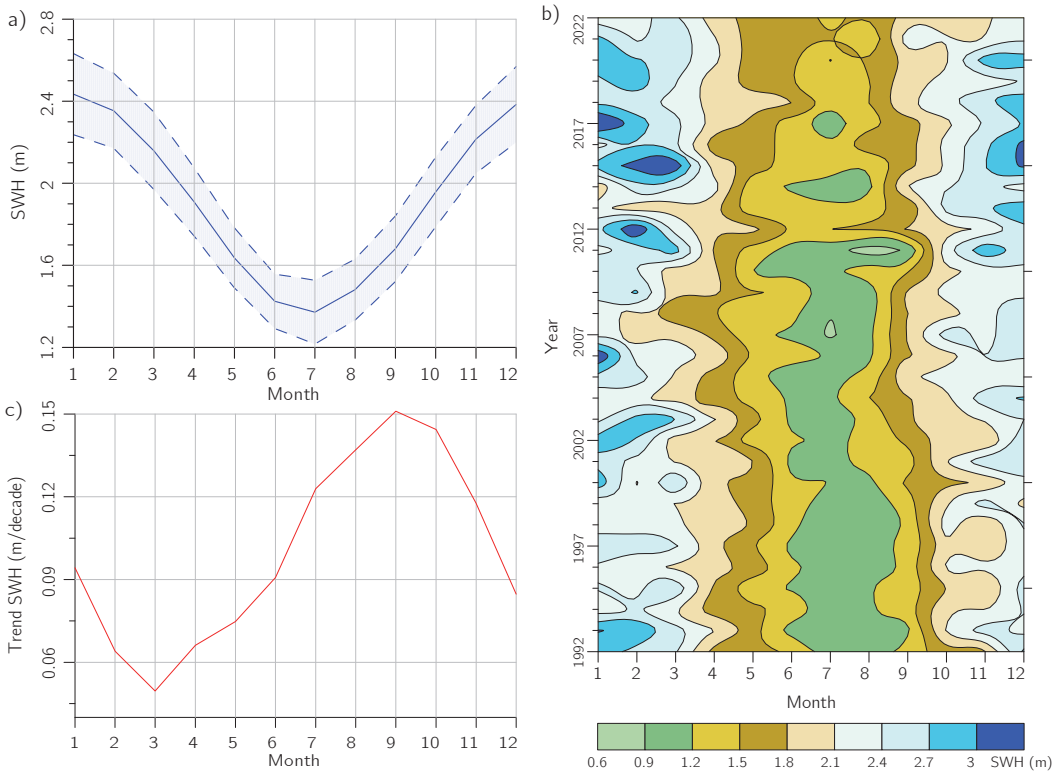

Figure 8. Seasonal and interannual (a, b) variability of the monthly average SWH and linear trend (c) in the Barents Sea, based on altimetry measurements combined into a single time series relative to ERS-1 satellite measurements for the period 1992–2021.

blow over the Barents Sea. In 1991–2021 we observed several cases when monthly mean SWH values exceeded 3 m – in 1993, 2006, 2012, 2015, 2016 and 2017. Since 2017, the maximum of the monthly mean SWH has been decreasing.

For the entire period from 1991 to 2021, the SWH distribution corresponds to the classical Rayleigh distribution. The SWH frequency maximum is observed at 1.25 m, while the maximal SWH is of 8 m, which is consistent with historical (1955–1985) ship observations (wave heights were 8–10 m) and probability calculations (they could have reached 11–13 m) [*Hydrometeorology…*, 1990].

For the period 1992–2021 the SWH general interannual trend was equal to $+0.10 \pm 0.06$ m/decade. Seasonal variability of SWH interannual trends varies from +0.05 m/decade in March to +0.15 m/decade in September. Values of SWH trends over +0.12 m/decade are observed from July to November which is explained by a steady interannual reduction of ice cover in the Barents Sea and by a significant increase in storm activity in the region.

According to [*Trofimov*, 2021], cases of storm anomalies in the Barents Sea are defined as the number of days with gale-force winds of 15 m/s or greater. In the Barents Sea, 15 storm days per year are considered as the statistical norm. While in 1992–1997 there were only 5 stormy days per year on average, in 2016–2022 this number increased to 65–75 days per year. Thus, significant changes in the atmospheric forcing seem to be the primary cause of SWH increase in the Barents Sea.

The obtained results show that, on the one hand, a significant reduction in ice cover in the Barents Sea allows ice-free navigation for a longer time per year, especially in Autumn, but on the other hand it increases wind fetch, which along with a significant increase in storm activity in the Barents Sea will lead to an increase of wind wave height in the sea. This will represent potential difficulties (and even danger) to navigation of ships designed for navigation in ice conditions and not intended for navigation in open waters of the world's oceans where large waves may be observed (e.g., icebreakers, barges, and other vessels).

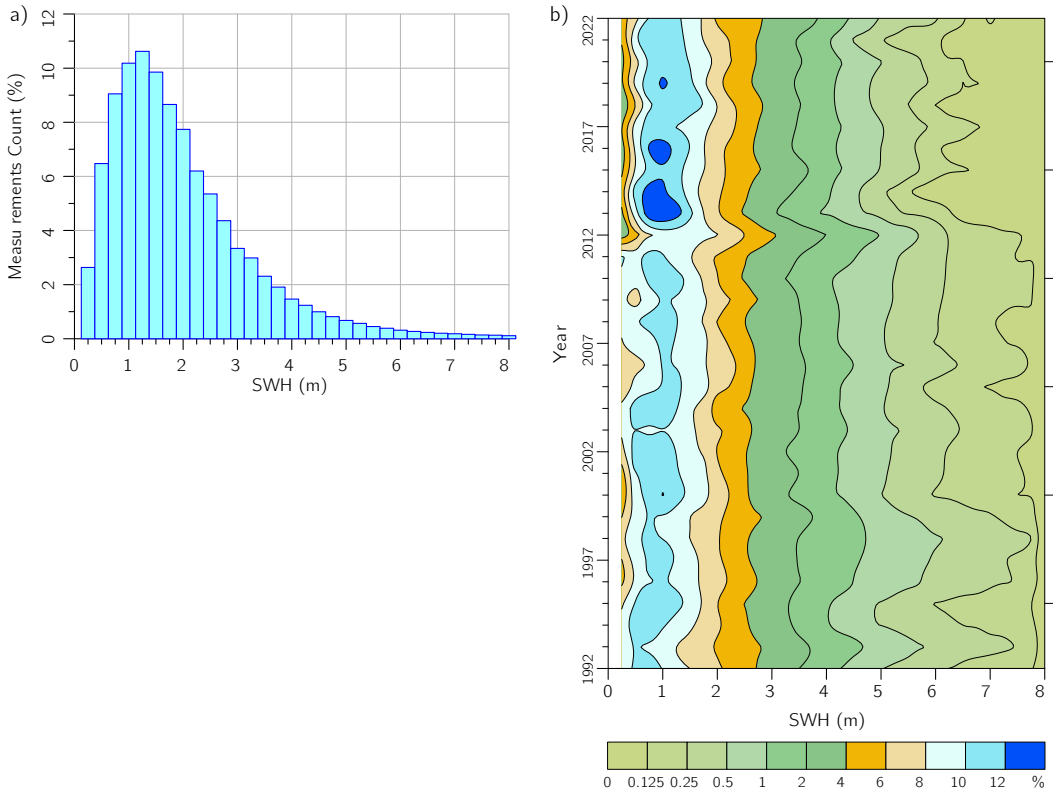

Figure 9. Distribution of SWH (m) in the Barents Sea, based on altimetry measurements combined into a single time series relative to ERS-1 satellite measurements for the period 1992–2021 as a percentage of the total number of measurements (a) and for each year (b).

Acknowledgments. This research was carried out within the framework of the Russian Science Foundation Grant 21-77-30010-P (2025–2027) "System analysis of geophysical process dynamics in the Russian Arctic and their impact on the development and operation of the railway infrastructure" https://rscf.ru/project/21-77-30010/.

References

Amarouche L., Thibaut P., Zanife O. Z., et al. Improving the Jason-1 Ground Retracking to Better Account for Attitude Effects // Marine Geodesy. — 2004. — Vol. 27, no. 1/2. — P. 171–197. — https://doi.org/10.1080/01490410490465210.

Atlas of Arctic / ed. by A. F. Treshnikov, E. S. Korotkevich, Yu. A. Kruchinin, et al. — Moscow : Main Directorate of Geodesy, Cartography under the Council of Ministers of the USSR, 1985. — 204 p. — (In Russian).

Brown G. The average impulse response of a rough surface and its applications // IEEE Transactions on Antennas and Propagation. — 1977. — Vol. 25, no. 1. — P. 67–74. — https://doi.org/10.1109/tap.1977.1141536.

Bué I., Lemos G., Semedo Á., et al. Assessment of satellite altimetry SWH measurements by in situ observations within 25 km from the coast // Ocean Dynamics. — 2024. — Vol. 74, no. 3. — P. 183–210. — https://doi.org/10.1007/s10236-024-01597-9.

Cabral I. S., Young I. R. and Toffoli A. Long-Term and Seasonal Variability of Wind and Wave Extremes in the Arctic Ocean // Frontiers in Marine Science. — 2022. — Vol. 9. — P. 802022. — https://doi.org/10.3389/fmars.2022.802022.

Collins C. O., Amador A., Babanin A., et al. Measuring Ocean Surface Waves [Preprint] // ESS Open Archive. — 2025. — https://doi.org/10.22541/essoar.175130482.28547248/v1.

Compo G. P., Whitaker J. S., Sardeshmukh P. D., et al. The Twentieth Century Reanalysis Project // Quarterly Journal of the Royal Meteorological Society. — 2011. — Vol. 137, no. 654. — P. 1–28. — https://doi.org/10.1002/qj.776.

Dumanskaya I. O. Regularities and features of ice conditions of the Barents Sea in the second half of XX - early XXI century // The Barents Sea System. — Moscow : Shirshov Institute of Oceanology Publishing House, 2021. — P. 179–194. — https://doi.org/10.29006/978-5-6045110-0-8/(15). — (In Russian).

Freeman E., Woodruff S. D., Worley S. J., et al. ICOADS Release 3.0: a major update to the historical marine climate record // International Journal of Climatology. — 2016. — Vol. 37, no. 5. — P. 2211–2232. — https://doi.org/10.1002/joc.4775.

Gavrikov A. V., Krinitsky M. A. and Grigorieva V. G. Modification of Globwave satellite altimetry database for sea wave field diagnostics // Oceanology. — 2016. — Vol. 56, no. 2. — P. 301–306. — https://doi.org/10.1134/s0001437016020065.

Good S., Fiedler E., Mao C., et al. The Current Configuration of the OSTIA System for Operational Production of Foundation Sea Surface Temperature and Ice Concentration Analyses // Remote Sensing. — 2020. — Vol. 12, no. 4. — P. 720. — https://doi.org/10.3390/rs12040720.

Grigorieva V. G. and Badulin S. I. Wind wave characteristics based on visual Observations and satellite altimetry // Oceanology. — 2016. — Vol. 56, no. 1. — P. 19–24. — https://doi.org/10.1134/s0001437016010045.

Gulev S. K. and Grigorieva V. G. Last century changes in ocean wind wave height from global visual wave data // Geophysical Research Letters. — 2004. — Vol. 31, no. 24. — https://doi.org/10.1029/2004gl021040.

Gulev S. K., Grigorieva V. G., Sterl A., et al. Assessment of the reliability of wave observations from voluntary observing ships: Insights from the validation of a global wind wave climatology based on voluntary observing ship data // Journal of Geophysical Research: Oceans. — 2003. — Vol. 108, no. C7. — P. 3236. — https://doi.org/10.1029/2002jc001437.

Hayne G. Radar altimeter mean return waveforms from near-normal-incidence ocean surface scattering // IEEE Transactions on Antennas and Propagation. — 1980. — Vol. 28, no. 5. — P. 687–692. — https://doi.org/10.1109/tap.1980.1142398.

Hydrometeorological conditions of the shelf zone of the seas of the USSR. Vol. 6. Barents Sea. Issue 3. South-eastern part of the sea / ed. by F. S. Terziev. — Leningrad : Gidrometeoizdat, 1985. — 273 p. — (In Russian).

Hydrometeorology and hydrochemistry of the seas of the USSR. Vol. 1. Barents Sea. Issue 1. Hydrometeorological conditions / ed. by F. S. Terziev, G. V. Girdyuk, G. G. Zykova, et al. — Leningrad : Gidrometeoizdat, 1990. — 279 p. — (In Russian).

Kostianoy A. G., Nihoul J. C. J. and Rodionov V. B. Physical Oceanography of the Frontal Zones in Sub-Arctic Seas. — Amsterdam : Volume 71 (Elsevier Oceanography Series). Elsevier Science, 2004. — P. 326.

Kuznetsova M. N. and Vasilyeva A. S. Transport Infrastructure of the Western and Central Arctic Regions of the Russian Federation: Analysis and Prospects // Arctic and North. — 2024. — No. 56. — P. 49–73. — https://doi.org/10.37482/issn2221-2698.2024.56.49.

Lebedev S. A. and Gusev I. V. Calibration of significant waves height altimetric measurements by wave reanalysis // Sovremennye problemy distantsionnogo zondirovaniya Zemli iz kosmosa. — 2022. — Vol. 19, no. 6. — P. 248–264. — https://doi.org/10.21046/2070-7401-2022-19-6-248-264.

Lebedev S. A., Kostianoy A. G., Ginzburg A. I., et al. Satellite Altimetry Applications in the Barents and White Seas // Coastal Altimetry. — Berlin : Springer Berlin Heidelberg, 2010. — P. 389–415. — https://doi.org/10.1007/978-3-642-12796-0_15.

Liu Q., Babanin A. V., Zieger S., et al. Wind and Wave Climate in the Arctic Ocean as Observed by Altimeters // Journal of Climate. — 2016. — Vol. 29, no. 22. — P. 7957–7975. — https://doi.org/10.1175/jcli-d-16-0219.1.

Lopatukhin L. I., Bukhanovsky A. V. and Chernysheva E. S. Reference data on the wind and wave regime of the shelf of the Barents and Kara Seas. — Saint Petersburg : Russian Maritime Register of Shipping, 2013. — P. 335. — (In Russian).

Lopatukhin L. I., Bukhanovsky A. V., Degtyarev A. B., et al. Reference data of wind and wave climate of the Barents Sea, the Sea of Okhotsk, and the Caspian Sea. — Saint Petersburg : Russian Maritime Register of Shipping, 2003. — P. 316. — (In Russian).

López-García P., Gómez-Enri J. and Muñoz-Pérez J. Accuracy assessment of wave data from altimeter near the coast // Ocean Engineering. — 2019. — Vol. 178. — P. 229–232. — https://doi.org/10.1016/j.oceaneng.2019.03.009.

Meucci A., Young I. R., Aarnes O. J., et al. Comparison of Wind Speed and Wave Height Trends from Twentieth-Century Models and Satellite Altimeters // Journal of Climate. — 2020. — Vol. 33, no. 2. — P. 611–624. — https://doi.org/10.1175/jcli-d-19-0540.1.

Mohamed B., Nilsen F. and Skogseth R. Interannual and Decadal Variability of Sea Surface Temperature and Sea Ice Concentration in the Barents Sea // Remote Sensing. — 2022. — Vol. 14, no. 17. — P. 4413. — https://doi.org/10.3390/rs14174413.

Myslenkov S. A., Golubkin P. A. and Zabolotskikh E. V. Evaluation of wave model in the Barents Sea under winter cyclone conditions // Lomonosov Geography Journal. — 2017. — No. 6. — P. 26–32. — (In Russian).

Myslenkov S. A., Platonov V. S., Toropov P. A., et al. Simulation of Storm Waves in the Barents Sea // Lomonosov Geography Journal. — 2015. — No. 6. — P. 65–75. — (In Russian).

Nesterov E. S. Extreme Waves in the Oceans and Seas. — Moscow, Obninsk : IG-SOTSIN, 2015. — P. 64. — (In Russian).

Nesterov E. S. Wind waves in the arctic seas (review) // Hydrometeorological research and forecasting. — 2020. — Vol. 3. — P. 19–41. — https://doi.org/10.37162/2618-9631-2020-3-19-41. — (In Russian).

Orimolade A. P. and Gudmestad O. T. On weather limitations for safe marine operations in the Barents Sea // IOP Conference Series: Materials Science and Engineering. — 2017. — Vol. 276. — P. 012018. — https://doi.org/10.1088/1757-899x/276/1/012018.

Reistad M., Breivik Ø., Haakenstad H., et al. A high-resolution hindcast of wind and waves for the North Sea, the Norwegian Sea, and the Barents Sea // Journal of Geophysical Research. — 2011. — Vol. 116, no. C5. — https://doi.org/10.1029/2010jc006402.

Rodionov V. B. and Kostianoy A. G. Oceanic Fronts of the North-European Basin Seas. — Moscow : GEOS, 1998. — 293 p. — (In Russian).

Serykh I. V. and Kostianoy A. G. Seasonal and Interannual Variability of the Barents Sea Temperature // Ecologica Montenegrina. — 2019. — Vol. 25. — P. 1–13. — https://doi.org/10.37828/em.2019.25.1.

Sharmar V. D., Tereschenkov V. P., Gavrikov A. V., et al. Moored Meteorological Buoy as Part of National Green-House Monitoring System in the Barents Sea // Oceanology. — 2025. — Vol. 65, no. 1. — P. 161–166. — https://doi.org/10.1134/s0001437024700772.

Timmermans B. W., Gommenginger C. P., Dodet G., et al. Global Wave Height Trends and Variability from New Multimission Satellite Altimeter Products, Reanalyses, and Wave Buoys // Geophysical Research Letters. — 2020. — Vol. 47, no. 9. — https://doi.org/10.1029/2019gl086880.

Trofimov A. G. The current trends in oceanographic conditions of the Barents Sea // Trudy VNIRO. — 2021. — Vol. 186, no. 4. — P. 101–118. — https://doi.org/10.36038/2307-3497-2021-186-101-118. — (In Russian).

Tsarau A., Guan C. and Shen H. H. Comparison of ice and wind-wave modules in WAVEWATCH III in the Barents Sea // Cold Regions Science and Technology. — 2020. — Vol. 172. — P. 103008. — https://doi.org/10.1016/j.coldregions.2020.103008.